Evolution of the magnetic properties of Co_2MnGa Heusler alloy films: From amorphous to ordered films

Y. V. Kudryavtsev and V. A. Oksenenko
Institute of Metal Physics, National Academy of Sciences of Ukraine, 252680 Kiev-142, Ukraine

Y. P. Lee,* Y. H. Hyun, J. B. Kim, J. S. Park, and S. Y. Park
q-psi and Department of Physics, Hanyang University, Seoul 133-791, Korea

J. Dubowik
Institute of Molecular Physics, Polish Academy of Sciences, 60-179 Poznań, Poland
(Received 1 December 2006; revised manuscript received 9 March 2007; published 24 July 2007)

We have investigated the evolution of the structural ordering and the crystal structure of polycrystalline Co_2MnGa Heusler alloy (HA) films and the structural effect on their magnetic properties. It is shown that the chemical and the structural ordering can be changed by the postannealing temperatures from an amorphous to more ordered structures typical for the HA. The magnetic properties of the films also depend strongly on the postannealing temperature. The as-deposited amorphous Co_2MnGa films show a weak ferromagnetic behavior due to the presence of a small amount of relatively highly magnetized regions in the nonmagnetic alloy matrix. Low-temperature (up to 513 K) annealing of the amorphous films results in the formation of a mixture of Co_2MnGa and metastable ϵ-Mn_3Ga and/or Mn_3Co_7 phases and causes a substantial increase in both magnetic moment and resistivity. Annealing at higher temperatures (up to 753 K) leads to a structural order of $A2/B2$ type. The amorphous $\rightarrow A2$ ($B2$) structural transformation in Co_2MnGa films induces an increase of about 30% in the alloy resistivity, qualitative changes in the shape of magneto-optical spectra, and an increase in the magnetic moment per f.u. up to $(2-2.5)\mu_B$. These results are discussed in terms of the band structure of the alloy. The best Co_2MnGa films, deposited on heated (753 K) substrates, exhibit the $B2$ (or $L2_1$) structure and nearly the bulk value of magnetization of $3.5\mu_B$.

DOI: 10.1103/PhysRevB.76.024430 PACS number(s): 75.70.−i, 76.50.+g, 78.20.Ls, 78.66.Bz

I. INTRODUCTION

Some full Heusler alloys (HAs) are ferromagnets and show 100% of spin polarization P due to a band gap for the minority-spin electrons at the Fermi level (E_F), which makes HA films attractive for applications in spintronics.[1–3] In particular, Co-based HAs have a high Curie temperature and a high magnetic moment[4,5] and might be used in spin-polarized current devices. However, the experimental values for P of Co-based HA films are smaller[6] than the theoretical perfect spin polarization, owing to the site or the atomic disorder. Therefore, much effort has been made to maximize P by improving the structural order of the HA films (see, for example, Ref. 7).

The effect of structural disorder on the electronic structure of HA is still a challenging problem. Especially, Orgassa *et al.* have shown that any kind of site disorder in NiMnSb HA results in decreases in the minority-spin energy band gap and P being nearly equal to zero at about 12% of the disorder.[8] Miura *et al.*[9] have shown that the $Co \leftrightarrow Cr$ disorder (i.e., the Cr atoms at the Co sites and vice versa) in Co_2CrAl HA significantly reduces the total magnetic moment and the spin polarization at E_F owing to the appearance of an intense peak of the Co $3d$ states, while the $Cr \leftrightarrow Al$ disorder gives practically no effect to the spin polarization. On the other hand, Co_2TiZ (Z=Al, Ga, Si, Ge, Sn, Sb) HA behaves in a different way: the $Ti \leftrightarrow Z$ type of disorder affects the electronic structure near the Fermi level.[10] Picozzi *et al.*[11] have shown that the Mn atoms at the Co sites in Co_2MnSi HA result even in an increase of the energy gap for the minority-spin subbands. It is also worth noting that the magnetic moment of Co_2FeAl has been found to be unaffected by the structural ordering.[12]

The effect of chemical disorder in HA is even more pronounced and has been also extensively investigated. It has been shown that a significant chemical disorder in amorphous Cu_2MnZ (Z=Al, In, Sn) HA films leads to a spin-glass behavior.[13] On the other hand, it was found that amorphous Ni_2MnZ (Z=In, Ga, Ge) (Refs. 14–16) and Cu_2MnAl (Ref. 17) HA films exhibit features of a Pauli paramagnet down to the liquid helium temperatures. Nakajima *et al.*[18] have observed a very small magnetic moment (lower than $0.001\mu_B$) in Co_2MnSi amorphous films and explained this in terms of the antiparallel coupling of the Co and the Mn amorphous subnetworks.

Co_2MnZ (Z=Sn, Si, Ge) HA films have been extensively investigated[16,18–25] and the results showed that the magnetic properties of these films depend strongly on the deposition and the postannealing temperatures and that the magnetization is usually lower than in the bulk. Co_2MnGa films have received less attention. Recent investigation on the magnetic and the electrical properties of Co_2MnGa HA films has given a saturation magnetization of $3.5\mu_B$/f.u. [~700 G (Ref. 26)] or less,[27] a remarkable strain-induced anisotropy,[26] and a relatively low spin polarization of ~50%.[28] According to the calculations of the electronic structure,[29] the Fermi level of Co_2MnGa is placed at the density-of-states (DOS) minimum of the minority states so that this alloy is at the verge of half-metallic behavior. In this paper, we show the structural

TABLE I. Structural and magnetic properties for Co_2MnGa films prepared on glass and mica substrates at various substrate (T_s) and annealing (T_a) temperatures. H_c=coercive field, ΔH=FMR resonance line width, and M_s=saturation magnetization.

Sample	Temperature (K)	Lattice parameter (nm)	Structure	Coherence length (nm)	M_s glass (G)	H_c		ΔH	
						Glass (Oe)	Mica (Oe)	Glass (Oe)	Mica (Oe)
Bulk		0.576	$L2_1$	55.0	750				
1	T_a=293	0.590	Amorphous	2.4	25	~50	~50	900	1500
2	513	0.581	Multiphase	23.2	245	164	382	800	900
3	598	0.579	$A2$	21.3	430	287	390	850	1300
4	728	0.579	$A2$ or $B2$	17.8	410	196	383	860	1250
5	723	0.583	$A2$ or $B2$	10.0		140			
6	T_s=753	0.580	$B2$ or $L2_1$	10.0	700	60		240	270

evolution of Co_2MnGa HA films when the amorphous films are annealed up to 750 K and the influence of structural and chemical disorder on their magnetic properties.

II. EXPERIMENTAL PROCEDURE

Bulk Co_2MnGa HA was prepared by melting Co, Mn, and Ga pieces of 99.99% purity together in an arc furnace with a water-cooled Cu hearth under an Ar atmosphere at a pressure of 1.3 atm. The Ar gas in the furnace was additionally purified by multiple melting of $Ti_{0.50}Zr_{0.50}$ alloy getter. To promote the volume homogeneity, the ingot was remelted five times. Weight loss after melting was not observed. The x-ray fluorescence analysis revealed an alloy composition of $Co_{0.494}Mn_{0.249}Ga_{0.257}$, i.e., close to Co_2MnGa. The alloy was then crushed to powders with a mean particle size of 80–100 μm. Co_2MnGa alloy films of 10×30 mm^2 in size and about 100 nm in thickness with different degrees of the structural order were prepared by flash evaporation onto glass, mica, and NaCl substrates simultaneously in a vacuum better than 2×10^{-5} Pa.

To obtain the Co_2MnGa films with the maximum possible disorder, we deposited them onto substrates cooled by liquid nitrogen. The as-deposited Co_2MnGa films were then subsequently annealed in series at 293 [i.e., at room temperature (RT)], 513, 598, 723, and 728 K, respectively, for 1 h in the high vacuum conditions. Additionally, some Co_2MnGa films were deposited onto substrates at 753 K. The structural characterization was carried out by using Θ-2Θ x-ray diffraction (XRD) with Cu $K\alpha$ radiation and field emission scanning electron microscopy (SEM) for the films deposited onto glass substrates, and by selective-area microdiffraction of transmission electron microscopy (TEM) for the films deposited and separated from the NaCl substrates. Selected samples were also investigated using the synchrotron radiation at Pohang Light Source (PLS). The various structural states of the Co_2MnGa alloy films annealed independently at 293, 513, 598, 728, and 723 K are referred to as 1, 2, 3, 4, and 5, respectively (see Table I). The structural properties of Co_2MnGa films after various stages of annealing are summarized in Table I.

The magnetic properties were investigated at RT by studying the angular dependencies of out-of-plane ferromagnetic resonance (FMR) at 9.3 GHz, as well as by measuring the magnetic hysteresis loops using a vibrating sample magnetometer (VSM). The effective magnetization (M_{eff}) and the g factor of ~2.0–2.05 were determined as parameters for fitting the experimental out-of-plane angular dependence of the resonance magnetic field, based on the Kittel relation. Additionally, the magneto-optical (MO) transverse Kerr effect (TKE) δ_p of the Co_2MnGa films was investigated at RT by the dynamical method using p-plane polarized light at an angle of incidence of 66° and in the spectral range of 360–1100 nm (3.40–1.05 eV). The electrical resistivity of the amorphous films were measured *in situ* in the temperature range from 150 to 800 K by employing the standard four-probe technique. Furthermore, the results of resistivity measurements were checked using the FMR and the magnetization measurements in the temperature range from 300 to 600 K.

III. EXPERIMENTAL RESULTS

The bulk Co_2MnGa HA sample, which was used for the film deposition, had the $L2_1$ structure with the lattice parameter a=0.5764 nm and $T_C\approx700$ K, close to those reported by Webster:[4] a=0.577 nm, $T_C\approx694$ K. Figure 1 shows the experimental XRD spectra for bulk and film 6 samples obtained at PLS, together with a simulated one of an ideally ordered Co_2MnGa alloy with the lattice parameter a =0.5764 nm and the $L2_1$ structure.

Vapor quenching deposition onto the cooled substrates leads to amorphous Co_2MnGa films, as evidenced by XRD and TEM (see Fig. 2). The amorphous Co_2MnGa films clearly exhibit a weak ferromagnetic [or superparamagnetic (SPM)] behavior at RT (Fig. 3), since the small remanence magnetization (~20 G) and the coercivity of ~50 Oe are comparable with the experimental noise.

The in-plane FMR spectrum of the amorphous Co_2MnGa film (Fig. 4) is broad with $\Delta H\simeq0.9-1.5$ kOe. Both large linewidth and low resonance field $H_{\text{eff}}\simeq2$ kOe indicate a rather inhomogeneous magnetic (and hence chemical) struc-

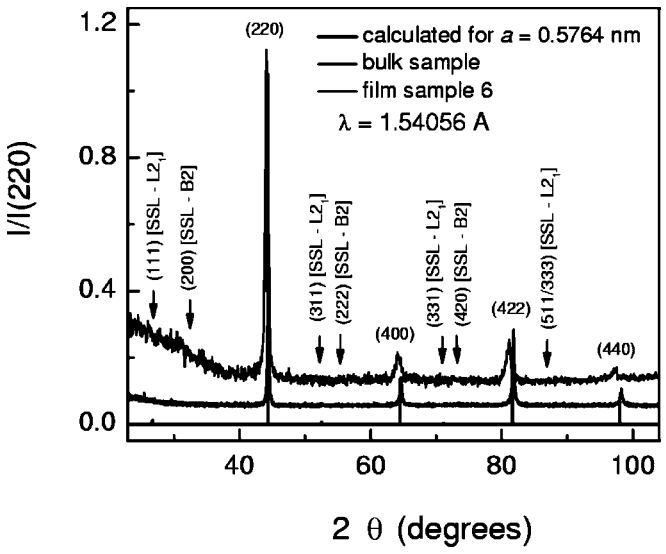

FIG. 1. Experimental XRD patterns of the Co_2MnGa samples (bulk and film 6), together with the simulated one for an ideally $L2_1$ ordered alloy. Arrows show the positions of the superstructure diffraction lines (SSL).

ture of the amorphous Co_2MnGa films. Very small MO response (data 1 in Fig. 5) in a wide range of the photon energy corresponds well to the weak ferromagnetic or SPM behavior. Interestingly, the magnetic behavior in the amorphous Co_2MnGa films at RT is different than in the amorphous Co_2MnSi films—they have been found to be paramagnetic at RT with a spin-glass behavior below 44 K.[21,30]

Low-temperature annealing at 513 K leads to crystallization (we will refer this annealing step to the $1 \rightarrow 2$ transformation), but as shown in Fig. 2, XRD pattern 2 consists, besides the main reflections characteristic of the $A2$ structure of Heusler alloys, of some additional peaks related to other phase(s) denoted by asterisks. A closer inspection of the TEM diffraction pattern of the film annealed at 438 K (Fig. 6) indicates that the transformation $1 \rightarrow 2$ results in decom-

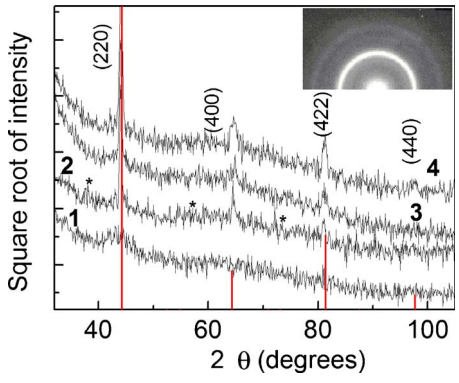

FIG. 2. (Color online) XRD diffraction patterns of the Co_2MaGa films deposited onto glass substrates at 150 K and then annealed in series at (1) 293, (2) 513, (3) 598, and (4) 728 K. Inset shows the TEM diffraction pattern of film 1, verifying its amorphous structure. The bars show the main diffraction peaks. Asterisk denote the peaks related to other phases (see text).

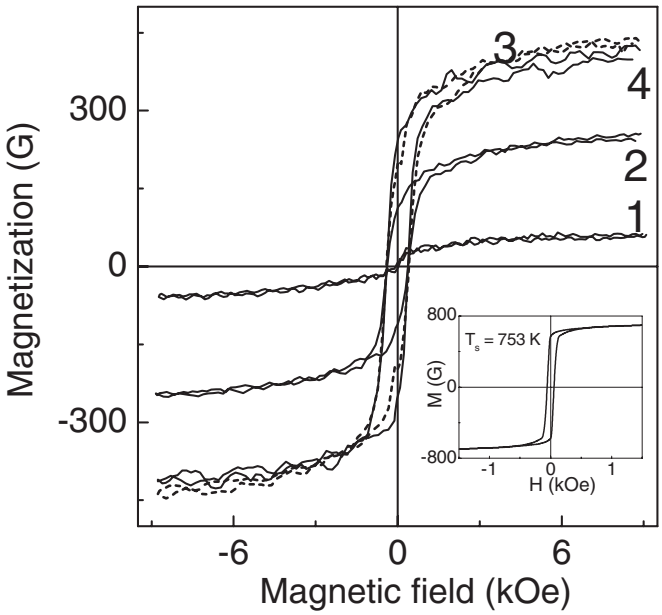

FIG. 3. In-plane room temperature magnetic hysteresis loops of the amorphous Co_2MaGa films deposited onto a mica substrate and annealed in series at (1) 293, (2) 513, (3) 598, and (4) 728 K. Inset shows the hysteresis loop of the film deposited at T_s=753 K.

position of the amorphous phase into the mixed Co_2MnGa and ϵ-Mn_3Ga (and/or Mn_3Co_7) phases. To have a better insight into the crystallization process of the amorphous Co_2MnGa films, we performed supplemental measurements of the electrical resistivity ρ, FMR, and magnetization as a function of temperature in the range of 300–600 K (800 K for ρ). Figure 7(a) shows clearly that at ~430 K, the electrical resistivity experiences a substantial jumplike increase and then at ~520 K, it decreases in a similar way but attains values by about 30% higher than those in the amorphous state. The resonance field H_r measured with the magnetic field applied perpendicular to the film plane also experiences

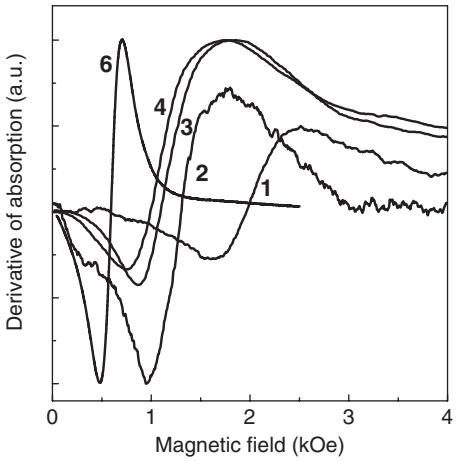

FIG. 4. FMR spectra of the amorphous Co_2MaGa films deposited onto a glass substrate and annealed in series at (1) 293, (2) 513, (3) 598, and (4) 728 K and deposited onto a glass substrate heated up to (6) 753 K. The spectra were taken with an in-plane applied field.

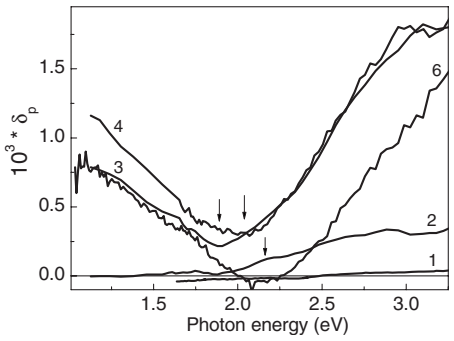

FIG. 5. TKE spectra of the amorphous Co_2MaGa films deposited onto a glass substrate and annealed at different temperatures: (1) 293, (2) 513, (3) 598, and (4) 728 K. The TKE spectrum of the Co_2MaGa film deposited onto a substrate heated up to 753 K is labeled with (6).

substantial changes in the same temperature range [Fig. 7(b)]. As shown in Fig. 7(c), the saturation magnetization M_{sat} does not change until about 500 K and then begins to increase to a value of 250 G in a range of 500–600 K. It is reasonable to conclude that crystallization of the amorphous films with nominal Co_2MnGa composition, occurring below ~520 K, leads to a strongly inhomogeneous polycrystalline structure. These results also suggest that both FMR and resistivity measurements are sensitive tools for tracing the chemical disorder in thin magnetic films. On the other hand, the $1 \rightarrow 2$ transformation leads to an enhancement of the magnetic characteristics of the Co_2MnGa films: the RT values of M_{eff} increase up to 500 G, $M_{sat} \simeq 250$ G, and the lattice parameter substantially decreases (see Table I and Fig. 8). Fine polycrystalline microstructure and chemical inhomogeneities bring about, however, a high coercivity of 160 Oe (or even 400 Oe for the films on mica substrate), a large FMR linewidth of 800–900 Oe, and a small MO response (see Figs. 3–5 and 8 and Table I). To conclude, annealing of the amorphous Co_2MnGa films at $T_a \leqslant 520$ K results in a mixed structure composed of fine polycrystalline $A2$ structure and ϵ-Mn_3Ga (and/or Mn_3Co_7) phases.

The next step of annealing of Co_2MnGa HA films at 598 K (i.e., $2 \rightarrow 3$ transformation) results in substantial changes in the shape of the TKE spectrum, as well as in an

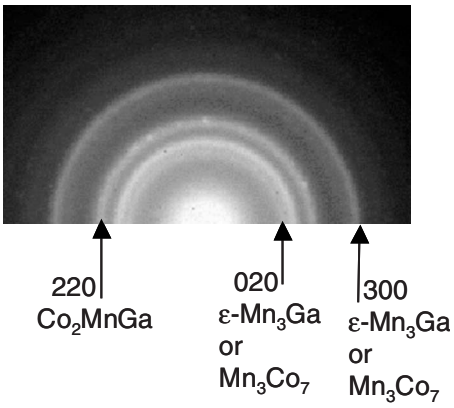

FIG. 6. TEM diffraction patterns of a Co_2MaGa film deposited at T_s=438 K.

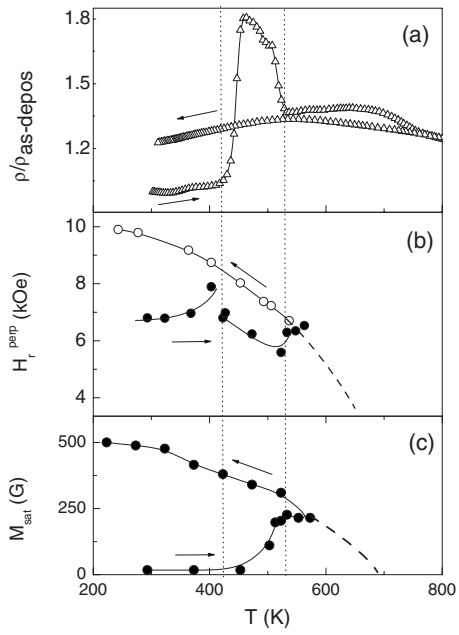

FIG. 7. Changes of (a) the electrical resistivity $\rho/\rho_{as\text{-}depos}$, (b) the FMR resonance field H_r^{perp}, and (c) the saturation magnetization M_{sat} in the course of heating and cooling back to RT of amorphous Co_2MaGa film.

increase of the value of the MO response δ_p (see data 3 in Fig. 5). Simultaneously, the resistivity ρ remains ~30% higher than that of the amorphous films [see Fig. 7(a)]. The $2 \rightarrow 3$ transformation is also accompanied by a twofold increase in M_{sat} to ~400 G $\approx M_{eff}$, which nicely corresponds to the changes in M_{sat} in the course of heating up to 600 K [see Fig. 7(c)]. It would suggest that the film annealed at 598 K is already magnetically homogeneous. Our XRD data presented in Fig. 2, with exclusively fundamental lines visible, do not allow us to make a reliable conclusion on the superstructural order of the Co_2MnGa in state 3. The TEM diffraction patterns of the film in state 3 shown in the upper panel of Fig. 9

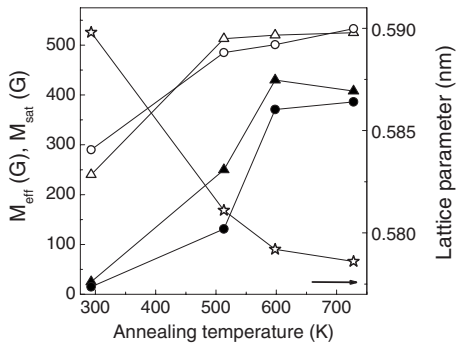

FIG. 8. Effect of annealing temperature on the effective (open symbols) and saturation (solid symbols) magnetizations determined from the FMR and the VSM measurements, respectively, for the Co_2MaGa HA films deposited onto mica (triangles) and glass (circles) substrates. Stars show lattice constants for the as-deposited and annealed Co_2MaGa films (right scale). Arrow indicates the lattice constant for bulk sample. The lattice constant for state 1 should be considered as the nearest interatomic distance.

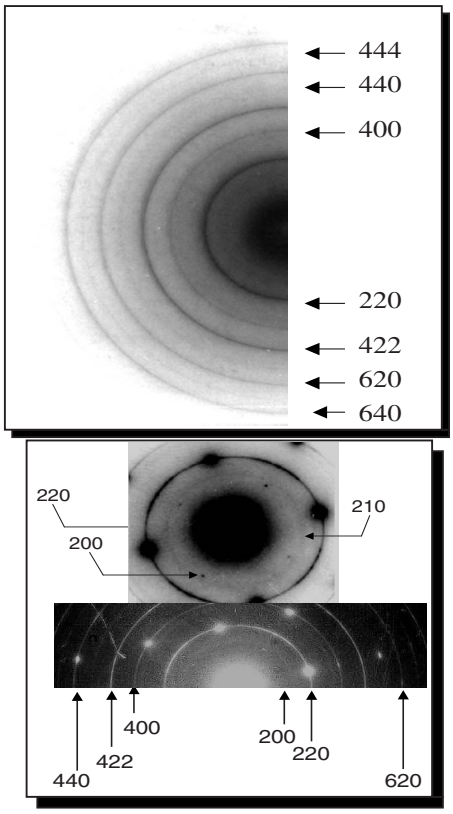

FIG. 9. Indexed electron diffraction patterns of the amorphous Co_2MaGa film (film 3) after annealing at 598 K (upper panel) and of the Co_2MaGa film deposited at T_s=753 K (bottom panel).

also indicate its fine polycrystalline microstructure with the fundamental reflections typical of the $A2$ structure. Therefore, our Co_2MnGa films in state 3 after annealing at 598 K possess at least the $A2$ HA structure with no traces of secondary phase(s). However, their electrical resistivity is always higher than that of the amorphous films. We should stress here that this unusual result (rechecked several times) is in clear contradiction to that for Co_2MnSi films, where crystallization of amorphous films caused a prominent drop in the alloy resistivity.[30]

The final step of annealing of the crystalline Co_2MnGa HA film samples at 728 K (i.e., $3 \rightarrow 4$ transition) practically does not change the TKE spectrum, M_{sat}, M_{eff}, and resistivity of the Co_2MnGa films (see Figs. 3–5 and 8). Therefore, the structure of our films in state 4 and their structural ordering do not differ much from that of state 3. However, a closer inspection of our better quality XRD data [Fig. 11(b)] of film 5 annealed at 723 K shows that besides the principal lines, there are also some traces of the superstructure lines (200), (420), and even (333), together with the visible (221) reflection, suggesting the presence of the $B2$ structure. Therefore, the films obtained on annealing at ~700 K (films 4 and 5) seem to be composed of mixed $A2$ and $B2$ structures. Moreover, the TEM diffraction (upper panel of Fig. 9) shows that the films obtained by postannealing of the amorphous ones are polycrystalline with the grain size of 20 nm with no or a very weak texture. The films obtained on the substrates heated up to ~700 K have much bigger grains of ~100 nm and are better ordered. The bottom panel of Fig. 9 shows the TEM diffraction patterns of film 6 deposited onto a NaCl(100) substrate at 753 K. Such films are partially epitaxial with the clearly visible (200) and (400) reflections besides the principal reflections. This suggests that such films possess the $B2$ or the $L2_1$ structure, resulting in their high magnetization of ~700 G (Table I), low coercivity (see inset in Fig. 3), and low FMR linewidth (Fig. 4). On the contrary, the annealed films in state 4 have significantly lower magnetization (~400 G), somehow lower than M_{eff} due to probably their polycrystalline microstructure and a significant influence of grain boundaries.

IV. DISCUSSION OF THE MAIN RESULTS

The formation of some residual magnetization in the amorphous Co_2MnGa films can be explained similarly to the case of the disordered CoAl and FeAl alloys. Equiatomic CoAl and FeAl alloys with $B2$ order are paramagnetic down to liquid helium temperatures.[31] However, in the disordered state, they are ferromagnetic at RT. The appearance of the ferromagnetic ordering in the disordered state of these alloys is thought to be due to the Co-rich (or Fe-rich) clusters in a nonmagnetic matrix.[32,33] We argue that the ferromagnetically ordered regions in the amorphous Co_2MnGa films also have the same origin, i.e., are related to the formation of Co-rich clusters with different numbers of Co atoms as the nearest neighbors in the nonmagnetic matrix. The appearance of Co-rich ferromagnetic clusters in the nonmagnetic matrix results in weakly ferromagnetic (or SPM) behavior at RT of the amorphous alloy.

A weak ferromagnetic behavior of the amorphous Co_2MnGa films is also confirmed by their weak MO response, as can be seen in Fig. 5. The shape of the TKE spectrum of the amorphous film shows some resemblance to that of Co films with strongly reduced TKE values.[34] Additionally, in the amorphous phase, there is a considerable (more than ten times) difference between the effective magnetization M_{eff} (evaluated from the FMR measurements) and magnetization saturation M_{sat} (obtained with VSM) of the amorphous films (see Fig. 6). In inhomogeneous magnetic films, M_{sat} represents the average volume magnetization, while M_{eff} is rather related to a configurational anisotropy of the Co-rich clusters[35] and may be as high as the maximal magnetization of the cluster if it has a disk shape. Therefore, a factor of 0.10 may be roughly regarded as a volume fraction of the ferromagnetic phase (i.e., Co-rich clusters) in a nonmagnetic matrix. According to the recent density-functional[29] studies of the electronic structures and exchange interaction parameters in Co_2MnX (X=Ga,Ge,Si), in the ordered Co_2MnGa with $L2_1$ structure, the Co atoms have a significant spin moment of $\sim 0.7\mu_B$ and the value of the local Mn spin moment is $\sim 3\mu_B$. Additionally, the Co-Mn interactions, though limited to the first neighbors, have been found to play an important role in the Co_2MnX HAs, making the magnetic short-range order effects operative even in the disordered structures.

Indeed, the SPM contribution to the total magnetization can be described by the Langevin law

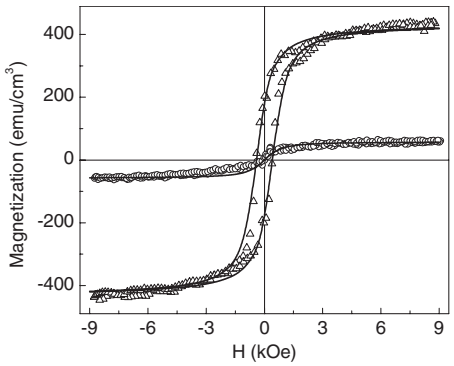

FIG. 10. Experimental (symbols) and simulated (lines) magnetization hysteresis loops for the Co_2MaGa films in states 1 (circles) and 3 (triangles).

$$M^{SPM} = M_s^{SPM} L(a), \tag{1}$$

where

$$L(a) = \coth(a) - 1/a. \tag{2}$$

M_{sat}^{SPM} is the saturation magnetization of the SPM phase and $a=\mu H/k_B T$.[36] μ is the magnetic moment of the Co-rich clusters, given by $\mu=M_s^{\text{Co}}\pi D^3/6$, where $\pi D^3/6$ is the volume of the clusters, assuming spheres with diameter D, and $M_{\text{sat}}^{\text{Co}}$ $=32.6$ A m^2/kg (or 290 emu/cm^3) is the effective magnetization of the clusters estimated from the FMR measurements. It is seen in Fig. 10 that the experimental magnetization hysteresis loop for the amorphous film (state 1) can be reasonably fitted using Eq. (1) with $D=2.1$ nm, i.e., with a magnetic cluster diameter of a few unit cells.

The XRD powder pattern for the ordered $L2_1$ structure yields, in addition to the fundamental reflections, also two types of superstructure diffraction lines. For the fundamental diffraction lines, h, k, l are all even and satisfy the condition $h+k+l=4n$. The superstructure reflections of the first type satisfy the condition $h+k+l=2n+1$, i.e., h, k, l are all odd [for example, the (111) reflection] and their intensities relative to the fundamental reflections reflect the presence of $Y \leftrightarrow Z$ type of disorder. The superstructure diffraction lines of the second type satisfy the condition $h+k+l=2n$ [for example, the (200) reflection] and their intensities relative to the fundamental reflections describe the $X \leftrightarrow Y(Z)$ type of disorder.[4] Thus, a $B2$ structure will appear for the case of $Y \leftrightarrow Z$ type of disorder and $A2$ one for $X \leftrightarrow Y(Z)$ type of disorder. In practice, it is very difficult to elucidate the ordering state of a ternary alloy only by XRD, since the scattering factors of $3d$ metals, Mn and Co, are practically the same (see, for example, Fig. 1). Therefore, an indirect information (for example, the structural dependencies of some physical properties) should be additionally employed to understand the actual type of structural order. Our x-ray measurements of polycrystalline films obtained by annealing at $T_a \geqslant 600$ K yielded only fundamental reflections (Fig. 2). This implies an $A2$ structure order. However, the results obtained with a better quality equipment (i.e., synchrotron radiation at PLS) showed that the films grown on a cold substrate and annealed at ~700 K had a mixed $A2/B2$ structure,

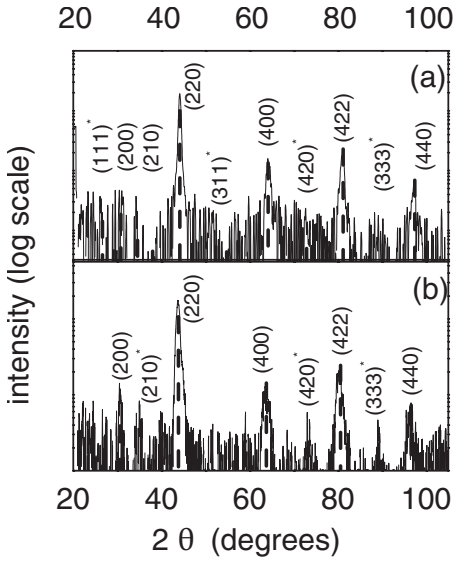

FIG. 11. X-ray diffraction patterns of the Co_2MaGa films: (a) deposited at $T_s=753$ K, (b) amorphous film annealed at T_a $=723$ K for 1 h. The bars show the calculated intensities for $B2$ [in (a)] and $A2$ [in (b)] structures. The indices denoted with asterisks are not well reproduced by the model.

whereas those grown on a heated substrate at 753 K showed a $B2/L2_1$ mixed structure [Fig. 11(a)]. Besides the XRD and the TEM results, our magnetic measurements showed a substantial increase in the magnetization in the range $600 \leqslant T_a \leqslant 700$ K with no substantial changes for $T_a > 700$ K. On the other hand, $M_{\text{sat}} \approx 400-500$ G is still lower than that for the bulk Co_2MnGa with $L2_1$ structure (700 G $\approx 3.5\mu_B$/f.u.)

Unlike the case of amorphous films, the polycrystalline Co_2MnGa films (states 2–4) show the full ferromagnetic behavior. According to an equation suggested by Stearns and Cheng,[37] the ferromagnetic contribution to the total magnetization is

$$M^{FM} = \frac{2M_s^{FM}}{\pi} \arctan\left[\frac{H \pm H_c}{H_c} \tan\left(\frac{\pi M_r}{2M_s^{FM}}\right)\right]. \tag{3}$$

In this expression, M_s^{FM} is the saturation magnetization, H_c the coercive field, and M_r the remanent magnetization. It seen (see Fig. 10) that the experimental $M(H)$ curve for the Co_2MnGa alloy film in, for example, state 3 is reasonably fitted using Eq. (3) and the experimental values of M_r, M_s^{FM}, and H_c with a negligible superparamagnetic contribution. This means that the polycrystalline Co_2MnGa alloy films are magnetically homogeneous.

On the other hand, our annealed films are polycrystalline with a grain size of 20 nm, and hence the grain boundaries seem to be an important factor for the magnetic properties. It has, for example, a strong influence on both the very broad FMR lines ($\Delta H \approx 900-1500$ Oe) and the high values of H_c of 200–400 Oe. The best films with a mixed $B2/L2_1$ structure obtained on the heated substrates have $\Delta H=200$ Oe, $H_c \approx 60$ Oe, and the highest magnetization of 700 G. To conclude, annealing of our amorphous films leads to polycrystalline films with $A2/B2$ structure with relatively small

grains and substantially lower magnetization than the bulk Co_2MnGa with $L2_1$ structure. The coherence length (Table I), estimated from the full width at half height of the most intensive (220) XRD reflection, experiences a decrease with the annealing temperature. This fact might be related to the preparation method (flash evaporation) rather than other factors such as film stress or phase segregation.

The main interest in our Co_2MnGa is their electronic band structure and the resulting transport properties. A good method to compare Co_2MnGa films with the recent results of theoretical band structure calculations is by measuring MO Kerr spectra over a wide range of photon energy. Although the Kerr spectrum does not provide a direct comparison of the electron band structure because of the absence of wave vector information, it is sensitive to small changes in the band structure. Therefore, if the theoretically calculated MO spectra share the same features as the experimental ones, we expect that the films share a similar band structure as that applied for the calculations. Figure 5 shows the MO spectra (data 3 and 4) obtained from the postannealed films 3 and 4. It is well known that optical and magneto-optical spectroscopies are rather sensitive for studying the electron energy structure of metals and alloys.[38] It is clearly seen that the TKE spectra for films 3 and 4 distinctly differ from those of films 1 and 2. At the same time, the shape and magnitude of the TKE spectrum for the $B_2/L2_1$ ordered film 6 much resemble those for films 3 and 4 with the only difference being that the increase in crystallinity of samples 3, 4, and 6 causes some consistent blueshift of the minimum (see Fig. 5). Furthermore, the off-diagonal components of the dielectric function for $B_2/L2_1$ ordered Co_2MnGa (determined from the experimental optical and MO data for sample 6) nicely agree with the results of first-principles calculations[39] (not shown). The detailed discussion of the effect of atomic disordering on the electronic structure of Co_2MnGa studied using optical and MO spectroscopy is the subject of a separate paper. However, it can be stated here that the resemblance between the shapes of the TKE spectra (and the off-diagonal components of the dielectric function) for the Co_2MnGa alloy films (samples 3, 4, and 6) and of the calculated spectrum for the $L2_1$ ordered alloy confirms their electronic (and hence atomic) structures.

We now attempt to interpret the influence of structure on the resistivity of Co_2MnGa alloy films. There are two striking anomalies in the effect of heat treatment on the resistivity of amorphous Co_2MnGa alloy films. These are (i) a clear jumplike anomaly in ρ vs T in the range of 420–520 K due to a phase separation [Fig. 8(a)] and, possibly, a strong electron spin-flip scattering on the SPM clusters and (ii) a noticeable (about 30%) increase in resistivity for the crystalline state, obtained by thermal cycling from 300 to 800 K and back to 300 K, in comparison with that of the as-deposited amorphous one. The typical values of the resistivity for the as-deposited amorphous Co_2MnGa films are 160–210 $\mu\Omega$ cm at RT. In the crystalline state, the resistivity is even larger. The estimated mean free path for as-deposited Co_2MnGa films does not exceed 1 nm and is comparable to the dimension of the magnetic clusters, giving rise to the spin-flip mechanism scattering. After annealing the amorphous Co_2MnGa films at $T_a \geqslant 600$ K, their magnetic structure becomes homogeneous and ferromagnetic. Therefore, the spin-flip contribution disappears.

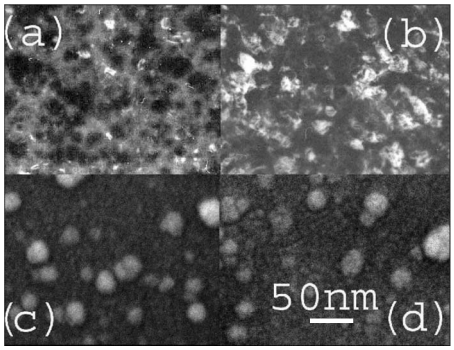

FIG. 12. [(a) and (b)] TEM and [(c) and (d)] SEM patterns for the Co_2MaGa films in [(a) and (c)] state 2 and [(b) and (d)] state 3, respectively.

At the same time, the mean free path of free carriers in the crystalline state is noticeably smaller than the mean grain size. Indeed, the TEM and SEM observations (see Fig. 12), as well as the estimation of coherent scattering length for x-ray diffraction (see Table I), showed nearly the same grain size in states 2 and 3. Therefore, we argue that the main origin of the enhanced ρ in the crystalline state with respect to the amorphous one is not related to the scattering at grain boundaries and may be due to another reason.

The resistivity described within the simple relaxation time τ approximation in a nearly free electron model (see, for example, Ref. 40),

$$\rho = \frac{m^*}{e^2 \tau n_{\text{eff}}} = \frac{3}{e^2 \tau v^2} \frac{1}{N(E_F)}, \tag{4}$$

where m^* and n_{eff} are, respectively, the effective mass and the effective density of conduction electrons per unit volume and v and $N(E_F)$ are the velocity and the DOS at the Fermi energy, has been shown[41] to depend on the long-range order (LRO) which affects both the scattering of the conduction electrons (i.e., τ) and the electron band structure $[N(E_F)]$ or n_{eff}. In the original Rossiter model,[41] the effect of LRO on both the electron scattering and the number of conduction electrons n_{eff} has been treated within the Bragg-Williams approximation, i.e., to describe the influence of a transition from an ordered to a disordered state in some binary alloys—Cu_3Au and Fe_3Al—on a temperature dependence of ρ. In our films, however, we deal with the opposite situation, i.e., with the transformation from the disordered to the ordered state. In most cases, such a transformation gives rise to an irreversible decrease in the resistivity with ordering, mainly due to an increase in τ. However, since τ has no reason to decrease with increasing order, the resultant increase in resistivity might be caused only by a decrease in n_{eff} or $N(E_F)$. The electronic structure of the Co_2MnGa compound has been calculated many times.[1–3,29,42–44] This compound actually is not pure half-metallic, however, P is pretty high because of the gap for minority bands and the Fermi level position intersecting only the tail of the occupied minority bands (see Fig. 2 in Ref. 3). The change in alloy symmetry from $L2_1 \rightarrow B2$

$\rightarrow A2$ type of order implies the disappearance of the Brillouin boundaries and gaps in the corresponding directions of the reciprocal space and an increase in $N(E_F)$.

V. CONCLUSIONS

The evolution of the structural ordering and the crystal structure of polycrystalline Co_2MnGa HA films were studied, and the effects on the magnetic properties were also elucidated. Postannealing leads to changes in the chemical and the structural ordering from an amorphous to more ordered structures typical for the HA. The magnetic properties are also varied correspondingly. A weak ferromagnetism is observed in as-deposited amorphous Co_2MnGa films, resulting from a small quantity of relatively highly magnetized regions in the nonmagnetic alloy matrix. Low-temperature (up to 513 K) annealing results in a structural mixture of Co_2MnGa and metastable ϵ-Mn_3Ga and/or Mn_3Co_7 phases, accompanied by significant growth of both magnetic moment and resistivity. The $A2/B2$-type structure is formed according to annealing at higher temperatures (up to 753 K), inducing an increase of about 30% in the alloy resistivity, modifications in the shape of magneto-optical spectrum, and an enhancement of the magnetic moment per f.u. up to $2-2.5\mu_B$. The anomalously increased resistivity was interpreted with the evolving energy band structure upon the structural ordering. The Co_2MnGa films, deposited on heated (753 K) substrates, is in the $B2$ (or $L2_1$) structure with a magnetization close to the bulk value.

ACKNOWLEDGMENTS

This work was supported by KOSEF through the Quantum Photonic Science Research Center, by MOST, Korea, and by Project No. 55/05-N of the national program "Nanomaterials" of the National Academy of Sciences of Ukraine. We are also grateful to A. E. Perekos, Y. N. Troshchenkov, Y. N. Petrov, and I. Gościańska for assistance and critical discussion.

*Corresponding author: yplee@hanyang.ac.kr

[1] S. Ishida, S. Sugimura, S. Fujii, and S. Asano, J. Phys.: Condens. Matter **3**, 5793 (1991).
[2] S. Fujii, S. Sugimura, S. Ishida, and S. Asano, J. Phys.: Condens. Matter **2**, 8583 (1990).
[3] I. Galanakis, P. H. Dederichs, and N. Papanikolaou, Phys. Rev. B **66**, 174429 (2002).
[4] P. J. Webster, Contemp. Phys. **10**, 559 (1969).
[5] K. H. J. Buschow, P. G. van Engen, and R. Jongebreur, J. Magn. Magn. Mater. **38**, 1 (1983), and references therein.
[6] W. H. Wang, M. Przybylski, W. Kuch, L. I. Chelaru, J. Wang, Y. F. Lu, J. Bartel, and J. Kirschner, J. Magn. Magn. Mater. **286**, 336 (2005).
[7] S. Kämmerer, A. Thomas, A. Hütten, and G. Reiss, Appl. Phys. Lett. **85**, 79 (2003).
[8] D. Orgassa, H. Fujiwara, T. C. Schulthess, and W. H. Butler, Phys. Rev. B **60**, 13237 (1999).
[9] X. W. Zhou, R. A. Johnson, and H. N. G. Wadley, Phys. Rev. B **69**, 144113 (2004).
[10] S. C. Lee, T. D. Lee, P. Blaha, and K. Schwarz, J. Appl. Phys. **97**, 10C307 (2005).
[11] S. Picozzi, A. Continenza, and A. J. Freeman, J. Magn. Magn. Mater. **272-276**, 315 (2004).
[12] N. Tezuka, S. Okamura, A. Miyazaki, M. Kikuchi, and K. Inomata, J. Appl. Phys. **99**, 08T314 (2006).
[13] L. Krusin-Elbaum, A. P. Malozemoff, and R. C. Taylor, Phys. Rev. B **27**, 562 (1983).
[14] Y. V. Kudryavtsev, Y. P. Lee, and J. Y. Rhee, Phys. Rev. B **69**, 195104 (2004).
[15] Y. V. Kudryavtsev, Y. P. Lee, and J. Y. Rhee, Phys. Rev. B **66**, 115114 (2002).
[16] V. A. Oksenenko, L. N. Trofimova, Y. N. Petrov, Y. V. Kudryavtsev, J. Dubowik, and Y. P. Lee, J. Appl. Phys. **99**, 063902 (2006).
[17] Y. V. Kudryavtsev, V. A. Oksenenko, N. N. Lee, Y. P. Lee, J. Y. Rhee, and J. Dubowik, J. Appl. Phys. **97**, 113903 (2005).
[18] K. Nakajima, G. Fen, C. Caillot, L. S. Dorneles, M. Venkatesan, and J. M. D. Coey, J. Appl. Phys. **97**, 10C904 (2005).
[19] U. Geiersbach, A. Bergmann, and K. Westerholt, J. Magn. Magn. Mater. **240**, 546 (2002).
[20] U. Geiersbach, A. Bergmann, and K. Westerholt, Thin Solid Films **425**, 225 (2003).
[21] S. Kämmerer, S. Heitmann, D. Meyners, A. Thomas, A. Hütten, and G. Reiss, J. Appl. Phys. **93**, 7945 (2003).
[22] L. S. Singh, Z. H. Barber, Y. Miyoshi, W. R. Branford, and L. F. Cohen, J. Appl. Phys. **95**, 7231 (2004).
[23] M. P. Raphael, B. Ravel, Q. Huang, M. A. Willard, S. F. Cheng, B. N. Das, R. M. Stroud, K. M. Bussmann, J. H. Claassen, and V. G. Harris, Phys. Rev. B **66**, 104429 (2002).
[24] A. Nefedov, J. Grabis, A. Bergmann, K. Westerholt, and H. Zabel, Physica B **345**, 250 (2004).
[25] T. Ambrose, J. J. Krebbs, and G. A. Prinz, J. Appl. Phys. **87**, 5463 (2000).
[26] M. J. Pechan, C. Yu, D. Carr, and C. J. Palmstrom, J. Magn. Magn. Mater. **286**, 340 (2005).
[27] E. Valerio, C. Grigorescu, S. A. Manea, F. Guinneton, W. R. Branford, and M. Autric, Appl. Surf. Sci. **247**, 151 (2005).
[28] S. N. Holmes and M. Pepper, J. Supercond. **16**, 191 (2003).
[29] Y. Kurtulus, R. Dronskowski, G. D. Samolyuk, and V. P. Antropov, Phys. Rev. B **71**, 014425 (2005).
[30] S. J. Kim, D. H. Lim, C. S. Yoon, and C. K. Kim, Solid State Commun. **132**, 361 (2004).
[31] D. J. Sellmyer, G. R. Caskey, and J. J. Franz, J. Phys. Chem. Solids **33**, 561 (1972).
[32] Yu. V. Kudryavtsev, Y. P. Lee, and K. W. Kim, J. Appl. Phys. **83**, 1575 (1998).
[33] Yu. V. Kudryavtsev, V. V. Nemoshkalenko, Y. P. Lee, and K. W. Kim, J. Appl. Phys. **82**, 5043 (1997).
[34] Y. P. Lee, R. Gontarz, and Yu. V. Kudryavtsev, Phys. Rev. B **63**, 144402 (2001).

[35] J. Dubowik, Phys. Rev. B **54**, 1088 (1996).
[36] A. Garcia Prieto, M. L. Fdez-Gubieda, C. Meneghini, A. Garcia-Arribas, and S. Mobilio, Phys. Rev. B **67**, 224415 (2003).
[37] M. B. Stearns and Y. Cheng, J. Appl. Phys. **75**, 6894 (1994).
[38] O. Hunderi, Thin Solid Films **37**, 275 (1976).
[39] S. Picozzi, A. Continenza, and A. J. Freeman, J. Phys. D **39**, 851 (2006).
[40] J. S. Dugdale, *The Electrical Properties of Disordered Metals* (Cambridge University Press, Cambridge, 1995).
[41] P. L. Rossiter, J. Phys. F: Met. Phys. **9**, 891 (1979).
[42] S. E. Kulkova, S. V. Eremeev, and S. S. Kulkov, Solid State Commun. **130**, 793 (2004).
[43] A. T. Zayak and P. Entel, J. Magn. Magn. Mater. **290-291**, 874 (2005).
[44] M. Y. Yablonskikh, Yu. M. Yarmoshenko, I. V. Solovyev, E. Z. Kurmaev, L.-C. Duda, T. Schmitt, M. Magnuson, J. Norgden, and A. Moewes, J. Electron Spectrosc. Relat. Phenom. **144-147**, 765 (2005).